A COMPARISON OF MODIFIED K-ε TURBULENCE MODELS FOR BUOYANT PLUMES

J. Worthy, V. Sanderson, and P. Rubini**

School of Mechanical Engineering, Cranfield University

Cranfield, Bedfordshire, MK43 0AL, UK

** Corresponding author

ABSTRACT

The effect of buoyancy on the production and dissipation of turbulent kinetic energy is investigated in variants of the popular k-ε turbulence model. The standard gradient diffusion model is considered for the scalar flux as well as a generalised gradient diffusion model. Also, the addition of the non-isotropic component of an algebraic stress model for the Reynolds stresses is assessed. The relative significance of the various models and terms are demonstrated using different combinations of the models, including the important flux Richardson correction term. The generalised gradient diffusion and algebraic stress models are shown to give a strong increase in turbulence production, although the effect on the flow can be largely controlled by the coefficient of the flux Richardson term. Recommendations are made regarding optimum models and coefficients.

NOMENCLATURE

B	buoyancy model term
$C_{various}$	various constants
g	gravity vector
G	production of turbulent kinetic energy due to buoyancy
k	turbulent kinetic energy
P	reduced pressure term (static – hydrostatic) / production turbulent kinetic energy due to shear
R_f	flux Richardson number
t	time
U	velocity
x	direction
β	thermal expansion coefficient
δ	Kronecker delta
ε	rate of dissipation of turbulent kinetic energy
μ	viscosity
φ	scalar
Φ	scalar
ρ	density

σ Prandtl number

subscripts

ASM from the algebraic stress model of buoyancy

B from the Boussinesq assumption

i,j,k vector direction

t time

0 reference point

superscripts

x' fluctuating value

$\overline{x}$ average value

INTRODUCTION

The Reynolds-averaged Navier-Stokes (RANS) equations are commonly employed as a basis for the solution of turbulent flows, although Large Eddy Simulation (LES) based approaches are increasingly used as significant computing resources become more readily available.

The process of Reynolds-averaging the Navier-Stokes and scalar transport equations introduces additional terms containing correlations of the fluctuating velocity components, which must themselves be modelled in order to effect closure. A large number of models have been proposed, many based on the Boussinesq assumption, which relates the Reynolds stresses to the mean velocity gradient via a turbulent viscosity. Typically these models have been classified into zero, one and two equation models, referring to the number of additional transport equations to be solved. Direct second moment closure models are also available, although these tend to be computationally more expensive and less robust and have consequently found less widespread application. The Boussinesq based two equation models have demonstrated a good balance between accuracy and efficiency. In particular, the k-ε turbulence model of Launder and Spalding [1] has been widely adopted, where transport equations are solved for the turbulent kinetic energy (k), and the rate of dissipation of the turbulent kinetic energy (ε).

Computational fluid dynamics (CFD) is being increasingly employed to investigate internal building flows, for heating, ventilation, and fire safety, where buoyancy effects due to thermal gradients become significant. Various authors have proposed and tested modifications of the standard turbulence models appropriate to buoyant flows, including

[2,3,4,5,6,7]. Initial developments utilised the standard Boussinesq gradient diffusion hypothesis (SGDH) to represent buoyancy induced turbulence generation, which has since been shown to be a significant component in the governing equations [2,3,4]. More recently, the general gradient diffusion hypothesis (GGDH) of Daly and Harlow [8] has been investigated, as has the algebraic stress model (ASM) of Davidson [5].

The effect of Richardson number, the ratio of buoyancy forces to inertial forces, is not well understood in the production of turbulence, so an empirical term, the flux Richardson term, was introduced into the ε equation to account for this. Rodi [3] gives what is now the standard format for this term.

Hossain and Rodi [2] demonstrated that the SGDH gave significant improvement over the standard k-ε model without a buoyancy model, although Shabbir and Taulbee [9] later found the axial heat flux to be inaccurately modelled with the SGDH.

Rodi [3] suggested that the coefficient of the flux Richardson term should vary between 0 and 1 dependent upon the flow. Markatos et al. [6] found the flux Richardson term to be insignificant in smoke simulations.

Davidson [5], and Yan and Holmstedt [7], found that the GGDH in conjunction with the ASM gave significantly improved results. Yan and Holmstedt [7] investigated these terms and found optimised values for the empirical constants when applied to a thermal plume.

The thermal plume represents an important benchmark simulation for any buoyant flow code as well as being a relevant flow in its own right, for example in atmospheric simulations, and fire simulations. Considerable experimental work has been carried out in this area, against which it is possible to validate turbulence models.

Chen and Rodi [4] gave an extensive review of the experimental work before 1980, and gave recommendations of the velocity and temperature spreading rates, and also centreline values. Later experiments including Papaniolaou and List [10], Shabbir and George [11], Ramprian and Chandrasekhara [12], and Sangras et al. [13], have found alternative values. These works [10,11,12,13] have questioned previously accepted plume statistics, complicating optimisation and selection of model components. However, the relative significance of the individual terms can be clearly demonstrated. Future optimisation may be eased with these considerations.

This paper follows the work of Yan and Holmstedt [7] and investigates the mechanics of the different models for buoyancy induced turbulence generation and dissipation in the k-ε model. The results of Chen and Rodi [4] are used for validation of the models, as applied to a thermal plume.

GOVERNING EQUATIONS

The density weighted Reynolds-averaged Navier-Stokes equations are given below. The pressure term represents the static pressure minus the hydrostatic pressure. The hydrostatic pressure is taken into account through the reference density.

$$\frac{\partial \rho}{\partial t} + \frac{\partial \left(\rho U_j\right)}{\partial x_j} = 0 \tag{1}$$

$$\frac{\partial \left(\rho U_i\right)}{\partial t} + \frac{\partial}{\partial x_j}\left(\rho U_i U_j\right) = -\frac{\partial P}{\partial x_i} + \frac{\partial}{\partial x_j}\tau_{ij} - \frac{\partial}{\partial x_j}\left(\rho \overline{u_i' u_j'}\right) + g_i\left(\rho - \rho_0\right) \tag{2}$$

$$\frac{\partial \left(\rho \Phi\right)}{\partial t} + \frac{\partial}{\partial x_j}\left(\rho \Phi U_j\right) = \frac{\partial}{\partial x_j}\left(\Gamma \frac{\partial \Phi}{\partial x_j}\right) - \frac{\partial}{\partial x_j}\left(\rho \overline{u_j' \varphi'}\right) \tag{3}$$

where $\tau_{ij} = \mu\left(\frac{\partial U_i}{\partial x_j} + \frac{\partial U_j}{\partial x_i}\right) - \frac{2}{3}\delta_{ij}\mu\frac{\partial U_k}{\partial x_k}$ (4)

The Reynolds stresses in the momentum equations must be modelled, as must the scalar fluxes, which using the Boussinesq assumption become:

$$-\rho\overline{u_i' u_j'} = \mu_t\left(\frac{\partial U_i}{\partial x_j} + \frac{\partial U_j}{\partial x_i}\right) - \frac{2}{3}\delta_{ij}\rho k \tag{5}$$

$$-\rho\overline{u_j' \varphi'} = \frac{\mu_t}{\sigma_t}\frac{\partial \Phi}{\partial x_j} \tag{6}$$

where the turbulent viscosity, μ_t, must be modelled, and the turbulent Prandtl number, σ_t, is typically a constant of O(1). This model of the scalar fluxes is referred to as the standard gradient diffusion hypothesis (SGDH) in this paper.

In the k-ε model the turbulent viscosity is defined as:

$$\mu_t = C_\mu \rho \frac{k^2}{\varepsilon} \tag{7}$$

where k is the turbulent kinetic energy, ε is the dissipation of the turbulent kinetic energy, and C_μ is a constant with a standard value of 0.09 [1].

The transport equations for k and ε are given by:

$$\frac{\partial(\rho k)}{\partial t} + \frac{\partial(\rho U_j k)}{\partial x_j} = \frac{\partial}{\partial x_j}\left(\frac{\mu_t}{\sigma_k}\frac{\partial k}{\partial x_j}\right) + \rho(P+G) - \rho\varepsilon \tag{8}$$

$$\frac{\partial(\rho \varepsilon)}{\partial t} + \frac{\partial(\rho U_j \varepsilon)}{\partial x_j} = \frac{\partial}{\partial x_j}\left(\frac{\mu_t}{\sigma_\varepsilon}\frac{\partial \varepsilon}{\partial x_j}\right) + C_{1\varepsilon}\frac{\varepsilon}{k}\rho(P+G)(1 - C_{3\varepsilon}R_f) - C_{2\varepsilon}\rho\frac{\varepsilon^2}{k} \tag{9}$$

where $P = -\overline{u_j' u_k'}\frac{\partial U_j}{\partial x_k}$ is the production of turbulent kinetic energy due to shear, $G = -\beta\overline{u_j' T'} g_j$ is the production of turbulent kinetic energy due to buoyancy, R_f is the flux Richardson number, $C_{3\varepsilon}$, an empirical correction term for the ε equation as defined by Rodi [3] for buoyant flows, and the thermal expansion coefficient is defined as $\beta = -(1/\rho)\frac{\partial \rho}{\partial T}$. The constants $C_{1\varepsilon}$ and $C_{2\varepsilon}$ are given the standard values of 1.44 and 1.92.

G can be formally derived in the k equation (see appendix 1). In the original k-ε model of Launder and Spalding [1], the turbulent production term was adopted in the modelled ε-equation, and has been included in a similar manner here. Amongst the earlier authors to use this format was Rodi [3].

This paper investigates the relative significance of the modelled production terms, P and G, and the flux Richardson term R_f.

BUOYANCY MODELS

The standard buoyancy modified k-ε model [2] uses the Boussinesq assumption in the P terms, and the SGDH model in the G terms.

$$P = P_B = \left(\frac{\mu_t}{\rho} \left(\frac{\partial U_j}{\partial x_k} + \frac{\partial U_k}{\partial x_j} \right) - \frac{2}{3} \delta_{ij} k \right) \frac{\partial U_j}{\partial x_k} \tag{10}$$

$$G = G_B = \beta \frac{\mu_t}{\sigma_t} \frac{\partial T}{\partial x_j} g_j \tag{11}$$

Shabbir and Taulbee [9] have shown that the axial heat flux (the flux perpendicular to the gravity vector) of the G term is considerably under-predicted when the SGDH is incorporated. This term is expected to have a significant effect on the spread rate of a thermal plume.

The general gradient diffusion hypothesis (GGDH) model was proposed by Daly and Harlow [8] as an alternative to the standard gradient diffusion model for the scalar fluxes. The model was derived from the second moment closure equations, and is defined by:

$$\overline{u'_j \varphi'} = -\frac{3}{2} \frac{C_\mu}{\sigma_\varphi} \frac{k}{\varepsilon} \overline{u'_j u'_k} \frac{\partial \Phi}{\partial x_k} \tag{12}$$

Using this model the G term becomes

$$G = G_G = \beta \frac{3}{2} \frac{C_\mu}{\sigma_t} \frac{k}{\varepsilon} \overline{u'_j u'_k} \frac{\partial T}{\partial x_k} g_j \tag{13}$$

Davidson [5] proposed an alternative model to the Boussinesq assumption for the Reynolds stress terms for buoyant flows, derived from the algebraic stress model of Rodi [3]. In this model the Reynolds stress tensor is split into two parts – that due to shear

production, which is again modelled with the Boussinesq assumption, and a non-isotropic part due to buoyancy. That is that $\overline{u'_j u'_k} = (\overline{u'_j u'_k})_{k-\varepsilon} + (\overline{u'_j u'_k})_{ASM}$ (14)

where $(\overline{u'_j u'_k})_{ASM} = \frac{k}{\varepsilon} \frac{(1-C_3)(B_{jk} - \frac{2}{3}\delta_{jk} B)}{C_1 + (P+B)/\varepsilon - 1}$ (15)

with $B_{jk} = -\beta \overline{u'_j T'} g_k - \beta \overline{u'_k T'} g_j$

$B = \frac{1}{2} B_{ll}$

The total P term including the ASM model is then given by

$$P_{ASM} = -\left(\frac{k}{\varepsilon} \frac{(1-C_3)(B_{jk} - \frac{2}{3}\delta_{jk} B)}{C_1 + (P_B + B)/\varepsilon - 1} \right) \frac{\partial U_j}{\partial x_k} \quad (16)$$

$$P = P_B + P_{ASM} \quad (17)$$

There are three ways of representing the scalar fluxes in the B term, in this model:

i) The SGDH (Eqn. 11).

ii) The GGDH with the Boussinesq assumption in the Reynolds stresses. (Eqns. 13,5).

iii) The GGDH with the ASM model incorporated into the Reynolds stresses. (Eqns. 13,14).

In a numerical scheme, the last becomes recursive, and can be implemented using the values from the previous iteration. All were tested, but only the first alternative, the SGDH, substituted back into the GGDH gave sensible results.

Rodi [3] found that the algebraic stress model showed no loss of accuracy when using the equilibrium assumption, where the production is equal to the dissipation. i.e $(P+G)/\varepsilon - 1 = 0$. This is assumed here also. In equation 15 this is $(P+B)/\varepsilon - 1 = 0$.

There is not a consistent literature on the flux Richardson term, R_f. The R_f term is the ratio of the rate of removal of energy by buoyancy to its production by the shear, $R_f = G/P$. [14]. An alternative definition given by Rodi [3] can be expressed as $R_f = G/(G+P)$, in conjunction with the empirical constant $C_{3\varepsilon}$ set to 0 in buoyant vertical shear layers and 1 in buoyant horizontal shear layers. Heindel et al. [15] let $C_{3\varepsilon} = \tanh(U/V)$ for mixed flows (where U is the local horizontal velocity, and V is the local vertical velocity). In the present work, the definition of Rodi [3] was employed with $C_{3\varepsilon}$ as a constant to be optimised.

The R_f term has previously been found to be insignificant in buoyant vertical shear flows. Markatos et al. [6] found that the G term in the k equation is far more important than the coefficient of the R_f term in fire simulations, and that buoyancy has no effect on the ε-equation. Cox [16] references Bos et al. [17] as finding the R_f term to have little effect, also in fire simulations. These findings have all used the standard buoyancy modified k-ε model.

This paper investigates the relative significance of the P and G terms using the above models for the Reynolds stress and scalar fluxes. The following combinations of the above models were tested. The acronyms are used throughout this work to refer to the various models.

ORIGINAL: The P term is modelled with the Boussinesq assumption, and the G term is not modelled and set to zero. The R_f term becomes zero in this case. $P=P_B$. G=0.

SGDH: This is the standard buoyancy modified k-ε model. The P term is modelled with the Boussinesq assumption and the G term uses the standard gradient diffusion hypothesis. $P=P_B$. $G=G_B$.

GGDH: The P term uses the Boussinesq assumption and the G term uses the general gradient diffusion hypothesis. $P=P_B$. $G=G_G$.

ASM: Davidson`s [5] algebraic stress model is applied. The G term is neglected. The P term is broken into the two parts; the $P_B$ (the Boussinesq part), and the $P_{ASM}$ (Davidson`s algebraic stress model part). $P=P_B+P_{ASM}$. $G=0$.

ASMSGDH: This is as the ASM model but the G term is modelled with the standard gradient diffusion hypothesis. $P=P_B+P_{ASM}$. $G=G_B$.

ASMGGDH: This is as the ASM model but the G term is modelled with the general gradient diffusion hypothesis. $P=P_B+P_{ASM}$. $G=G_G$.

For the ASM term, the SGDH model has been re-substituted back into the remaining Reynolds stress terms. Only terms in the k and ε equations were modelled. The Reynolds stresses in the RANS equations were modelled in all cases using the Boussinesq assumption.

NUMERICAL IMPLEMENTATION AND SIMULATIONS

The numerical simulations were carried out using the code SOFIE (Simulation of Fires in Enclosures), specifically developed at Cranfield for compartment fire predictions [18,19]. SOFIE is based upon a finite volume procedure utilising an underlying general non-orthogonal coordinate system with co-located velocities, momentum smoothing and a pressure correction algorithm. Dependent variable interpolation has a choice of schemes. A second order accurate TVD scheme was used in this work.

The planar plume was simulated in a rectangular domain of 2m base by 2.7m height, with a 0.06m entrance width. For speed of calculation a mirror symmetry boundary was used along the centreline of the plume. A solid wall boundary was specified at the bottom of the domain. Static pressure boundaries were employed on the remaining boundaries, allowing flow into and out of the domain.

At the plume source, inflow velocity was specified as 0.01m/s with small values (1.0e-6) for the turbulent kinetic energy and dissipation rates and a temperature of 1000K.

Flow into the calculation domain across the static pressure boundaries was specified with a fixed temperature of 298.15K, turbulent intensity of 0.5%, and turbulent length scale of 0.01m. Flow out is evaluated to ensure local continuity at the boundary cells.

The computational grids were uniformly spaced across the plume entrance, and uniformly spaced along the remainder of the horizontal axis, with a single uniform grid spacing in the vertical axis. Four grid distributions were used, labelled A, B, C, D. Unless otherwise stated grid A was used. Grid A had 4+50x50 cells where there are 4 cells

across the plume source and 50 cells across the rest of the base of the domain. B, in a similar manner, had 4+70x70 cells, C had 6+100x100 cells, and D had 10+200x150 cells.

PLANAR PLUMES

Chen and Rodi [4] presented a detailed review of experimental data up to 1980, and recommended spreading rates of 0.12 measured by the velocity half-width and 0.13 for the temperature spread measured by its half-width. These figures are frequently used as the reference data with which to optimise models (Yan and Holmstedt [7], Hossain and Rodi [2]). Spread rates are measured in terms of the half width where the half-width in each case is defined to be that distance from the centre where the value (velocity or temperature here) is half of its centreline value. Values ranging from 0.08 to 0.147 for velocity spread and from 0.098 to 0.14 for the temperature spread were reported by Chen and Rodi [4]. More recent experiments have supported these values. Ramaprian and Chandrasekhara [12] found a velocity spread of 0.11 and temperature spread of 0.13. Sangras et al. [13] found even lower values.

The velocity centreline values can be clearly evaluated for the planar case, since the velocity centreline asymptotes to a constant value away from the source. Different authors give different values again. For this configuration Chen and Rodi [4] would have given a maximum velocity of 0.31m/s, Ramprian and Chandrasekhara [12] of 0.34m/s, and Rouse [20] of 0.29m/s.

The cross-stream profile of any characteristic variable (such as velocity or temperature) has been empirically shown to approximate a Gaussian (normal) distribution. Empirical constants and terms can be altered to suit the experimental data as will be shown.

RESULTS

Preliminary solutions were obtained to quantify grid dependence, and secondly to confirm that the plume spread rates were genuinely evaluated in the self-similar region.

Grid independence was demonstrated using the ASMGGDH model on four grids, as shown in Table 1. This shows a tendency for a very slight increase in spread rates with grid refinement. The change is sufficiently small to be considered grid independent. Grid independence was also shown for the SGDH model, and the other models were assumed to be grid independent from these. Based on these comparisons grid A was used for model evaluation in the following sections.

The self-similarity and Gaussian distributions of the characteristic profiles are shown in Figures 1 and 2. The overlapping curves demonstrate that the plume has adopted a self-similar profile in this region. The curves are normalised in the vertical axis to the centreline velocities and in the horizontal axis with the distance to the half-centreline velocity.

It is important that the spreading rate is determined in the self-similar region. Table 2 presents results from the models with $C_{3\varepsilon}$, the coefficient of the flux Richardson number, fixed at 0.6, as recommended by Yan and Holmstedt [7], whose initial work this follows. The spread rates were evaluated using the half-width, both at a vertical distance between 1m and 2m from the source, representing the self-similar region as demonstrated

previously, and between the source (0m) and 2m from the source. As the results demonstrate, misleading conclusions can be drawn if the inappropriately specified spread rate is utilised. Spread rates are evaluated in the self-similar region throughout the remainder of this paper.

Table 3 demonstrates that the SGDH model shows no or little improvement on the ORIGINAL model. This is because the value of the SGDH term is small as can be seen in Figure 3. This is contrary to results given by Hossain and Rodi [2] who show the SGDH to be a great improvement on the ORIGINAL model. This could be due to the method of evaluation of spread rates as demonstrated in Table 2. If the spread rates are measured from the source, then there is the appearance of good improvement. The effect of the SGDH model is for the plume to widen rapidly at the source before settling into the self-similar region, where the spread rate is not altered by the SGDH model as compared to the ORIGINAL model.

The R_f term, when in conjunction with the SGDH model, has previously been found to have little effect (Markatos et al. [6], Bos et al. [16]). This work is in agreement with these findings. It makes sense that the R_f term has little effect with the SGDH model since G_B is almost negligible. Markatos [6] suggests removing the G term from the ε equation altogether. This is equivalent to letting $C_{3\varepsilon}$ equal unity. It would still make little difference to the SGDH model, but the GGDH and ASM would be affected it as shown below.

It is clear from the results shown in Table 2 that the GGDH and ASMGGDH models gave the most significant increases in spread rates. Conversely, the SGDH, ASM, and ASMSGDH showed little increase on ORIGINAL (the unmodified k-ε model), indicating the significance of the GGDH model assumption.

Figure 4 shows the relative magnitude of the production terms in the k-equation for the ASMGGDH model. It can be seen that the overall production is increased by about 25%, over half of which is generated by the P_{ASM} term. The magnitude of the P_{ASM} term was found to be similar in the ASM model even though there is no comparable increase in the spread rates. This difference is attributed to the controlling effect of the buoyancy production term in the ε-equation and the R_f multiplier.

The effect of the flux Richardson term, R_f, is to decrease the turbulent dissipation rate with increasing buoyancy, resulting in an overall increase in the net turbulence production, and hence increase the spread rate. In the ASM model the R_f term is 0 by definition (since G is not modelled), whereas in the ASMGGDH the value is approximately 0.15. This implies that overall, the R_f term in the ε-equation has considerably more direct effect than the production terms in both the k and ε equations.

The results from the GGDH model were also significantly affected by the R_f term. Table 4 shows the variation of spread rates of the GGDH and the ASMGGDH models with $C_{3\varepsilon}$ varying.

When $C_{3\varepsilon}$ is 0.7 the two models give equivalent results. The P_{ASM} term in the ASMGGDH model can be considered to be a damping function on the R_f term in the GGDH model around this value. This makes sense since adding the P_{ASM} term into the R_f term decreases the value of the R_f term.

Table 5 gives the centreline velocities for the ASMGGDH and GGDH models, again with $C_{3\varepsilon}$ varying. There is little difference between the two models and both models predict these values qualitatively correctly. i.e. the greater the spread rate, the less the velocity, keeping the buoyancy flux constant at all distances from the source. The models are equivalent for the spreads and the maximum velocity with $C_{3\varepsilon}$ = 0.7. These fit Chen and Rodi's [4] proposed values well.

Whilst the ASMGGDH gives no advantage over the GGDH in this simulation, it does not increase the computing time by any significant margin and may offer benefits for other flows. The ASM can be used in the momentum equations also, although Yan and Holmstedt [7] found this unstable in the simulation of buoyant fire plumes.

CONCLUSIONS

The results from the present work have confirmed that for a plane plume the SGDH model makes very little difference to the spread rates in comparison to the ORIGINAL model, although the plume does expand more rapidly in the near field of the source before the self-similar region.

The primary positive conclusion drawn from this work is that the GGDH and ASMGGDH models in conjunction with the R_f term give significantly improved results over the ORIGINAL and also the SGDH model, and that the R_f term is a necessary factor for this improvement. Furthermore, that greatest contribution to this improvement can be attributed to the use of the GGDH to model the scalar fluxes in the buoyancy production term combined with the R_f term. The ASM model has a beneficial effect in conjunction with the GGDH and R_f but does not offer any significant improvement when used by itself. Rodi [3] recommends not using the R_f term for vertical shear flows. However, in combination with the above models it has been found to be very important, to the extent that without it the GGDH and ASMGGDH models would show very little improvement.

Chow and Mok [21] investigated a number of buoyancy models including the ASMGGDH model in fire simulations. They found it offered no significant improvement upon the SGDH model. This is in agreement with these results since they did not incorporate the flux Richardson number.

Optimal values for $C_{3\varepsilon}$ can be given for each model depending on which experimental data is used, and 0.7 is found for the GGDH and ASMGGDH using the data of Chen and Rodi [4]. However, using the more recent data, for example [13], then the ORIGINAL and SGDH models give reasonably accurate results, suggesting that the use of the R_f term with the GGDH and ASM models is not necessary to improve the spread rates. Consistent experimental data is needed to truly optimise relevant coefficients.

APPENDIX 1

Derivation of the k-equation with buoyancy terms. For simplicity, the incompressible equations are used.

Let

$$\mathrm{N}_i = \rho\frac{\partial u_i}{\partial t} + \rho u_k \frac{\partial u_i}{\partial x_k} + \frac{\partial p}{\partial x_i} - \mu\frac{\partial^2 u_i}{\partial x_k \partial x_k} - g_i(\rho - \rho_0) = 0$$

be incompressible momentum equations with buoyancy terms. Let

$$\mathrm{N}_i{}^a = \rho\frac{\partial U_i}{\partial t} + \rho U_k \frac{\partial U_i}{\partial x_k} + \frac{\partial P}{\partial x_i} - \mu\frac{\partial^2 U_i}{\partial x_k \partial x_k} + \rho\frac{\partial \overline{u_i' u_k'}}{\partial x_k} - g_i(\widehat{\rho} - \rho_0) = 0$$

be the Reynolds-averaged incompressible momentum equations.

Take moments about each equation and subtract in this manner:

$$\overline{u_i'\mathrm{N}_i - u_i'\mathrm{N}_i{}^a} = 0$$

Take each part of the summed equation in turn.

Time derivatives:

$$\begin{aligned}\overline{u_i'\rho u_{i,t} - u_i'\rho U_{i,t}} &= \overline{u_i'\rho u_{i,t}'} \\ &= \frac{1}{2}\rho\overline{u_i'^2{}_{,t}} \\ &= \rho\frac{\partial k}{\partial t}\end{aligned}$$

Convection terms:

$$\overline{u_i'(U_k + u_k')\rho(U_i + u_i')_{,k} - u_i' U_k \rho U_{i,k}} = \overline{u_i' U_k \rho u_{i,k}'} + \overline{u_i' u_k' \rho U_{i,k}} + \overline{u_i' u_k' \rho u_{i,k}'}$$

$$= U_k \tfrac{1}{2}\rho\overline{(u_i'^2)_{,k}} + \overline{u_i' u_k'}\rho U_{i,k} + \overline{u_k'\rho\tfrac{1}{2}(u_i'^2)_{,k}}$$

$$= U_k \rho k_{,k} + \overline{u_i' u_k'} \rho U_{i,k} + \overline{u_k' \rho \tfrac{1}{2}(u_i'^2)_{,k}}$$

$$= \rho U_k \frac{\partial k}{\partial x_k} + \rho \overline{u_i' u_k'} \frac{\partial U_i}{\partial x_k} + \frac{\partial}{\partial x_k}(\tfrac{1}{2} \rho \overline{u_k' u_i'^2})$$

Note: $\overline{u_k' \rho \tfrac{1}{2}(u_i'^2)_{,k}} = \overline{\tfrac{1}{2} \rho (u_k' u_i'^2)_{,k}} - \overline{\tfrac{1}{2} \rho u_{k,k} u_i'^2}$

$$= \overline{\tfrac{1}{2} \rho (u_k' u_i'^2)_{,k}}$$

Pressure terms:

$$\overline{u_i'(P + p')_{,i} - u_i' P_i} = \overline{u_i' p'_{,i}}$$
$$= \overline{(u_i' p')_{,i}} - \overline{u_{i,i}' p'}$$
$$= \overline{(u_i' p')_{,i}}$$
$$= \frac{\partial}{\partial x_i}(\overline{u_i' p'})$$

Viscous diffusion terms

$$\overline{u_i'(\mu(U_i + u_i')_{,k} - \mu U_{i,k})_{,k}} = -\overline{u_i' \mu u_{i,k^2}'}$$

$$= -\tfrac{1}{2}(u_i'^2)_{,k^2} + \mu \overline{u_{i,k}'} \overline{u_{i,k}'}$$

$$= -\mu \frac{\partial^2 k}{\partial x_k^2} + \mu \overline{\frac{\partial u_i'}{\partial x_k}} \overline{\frac{\partial u_i'}{\partial x_k}}$$

Turbulent stress terms:

$$\overline{0 - u_i'(\rho \frac{\partial \overline{u_i' u_k'}}{\partial x_k})} = -\overline{u_i' \rho \frac{\partial \overline{u_i' u_k'}}{\partial x_k}} = 0$$

Buoyancy terms:

$$\overline{-u_i' g_i(\bar{\rho} + \rho' - \rho_0) + u_i' g_i(\bar{\rho} - \rho_0)} = -g_i \overline{u_i' \rho'}$$

$$= -g_i \overline{u_i' \rho_{,t} T'}$$

$$= -g_i \frac{\partial \rho}{\partial T} \overline{u_i' T'}$$

$$= g_i \beta \overline{u_i' T'} \rho$$

Assembling all the terms gives:

$$\rho \frac{\partial k}{\partial t} + \rho U_k \frac{\partial k}{\partial x_k} = \mu \frac{\partial^2 k}{\partial x_k \partial x_k} - \mu \overline{\frac{\partial u_i'}{\partial x_k} \frac{\partial u_i'}{\partial x_k}} - \overline{\frac{\partial}{\partial x_i} u_i' p'} - \overline{\frac{\partial}{\partial x_k} \rho u_i'^2 u_k'} - \rho \overline{u_i' u_k'} \frac{\partial U_i}{\partial x_k} - \rho \beta \overline{u_i' T'} g_i$$

The first three terms are recognisable as the standard terms in a transport equation. The time derivative, the convection and the diffusion of k. The next term is modelled by the dissipation rate, ε. The pressure term and the triple correlation are modelled and added to the regular diffusion term to make the turbulent diffusion term. The final terms are the production due to shear, P, and the production due to buoyancy, G, respectively.

Use has been made of $\frac{\partial u_j'}{\partial x_j} \approx 0$.

REFERENCES

1. B. E. Launder, D. B. Spalding, The numerical Computation of Turbulent Flows, Comput. Meth. Appl. Mech. Eng., vol. 3, pp. 269-289, 1974.
2. M. S. Hossain, W. Rodi, A Turbulence Model for Buoyant Flows and its Application to Vertical Buoyant Jets, in Turbulent Buoyant Jets and Plumes, 1982.
3. W. Rodi, Turbulence Models and their Applications in Hydraulics-A State of the Arts Review, University of Karlsruhe, Germany, 1984.
4. J. C. Chen, W. Rodi, Turbulent Buoyant Jets: a review of experimental data, HMT, vol.4, Pergamon, 1980.
5. L. Davidson, Second-order correction of the k-ε model to account for non-isotropic effects due to buoyancy, Int. J. Heat Mass Transfer, vol. 33, pp. 2599-2608, 1990.
6. N. C. Markatos, M. R. Malin, G. Cox, Mathematical Modelling of Buoyancy-induced Smoke Flow in Enclosures, Int. J. Heat Mass Transfer, vol. 25,no. 1, pp. 63-75, 1982.
7. Z. Yan, G. Holmstedt, A two-equation model and its application to a buoyant diffusion flame, Int. J. Heat Mass Transfer, 1998.
8. B. J. Daly, F. H. Harlow, Transport equations of turbulence, Physics Fluids, vol. 13, pp. 2634-2649, 1970.
9. A. Shabbir, D. B. Taulbee, Evaluation of Turbulence Models for Predicting Buoyant Flows, J. Heat Transfer, vol. 112, pp. 945-951, 1990.
10. P. N. Papanicolaou, E. J. List, Investigation of Round Vertical Turbulent Buoyant Jets, J. Fluid Mech., vol. 209, pp. 151-190, 1988.
11. A. Shabbir, W. K. George, Experiments on a Round Turbulent Buoyant Plume, NASA Technical Memorandum 105955, 1992.
12. B. R. Ramaprian, M. S. Chandrasekhara, Measurements in Vertical Plane Turbulent Plumes, J. Fluids Engineering, vol. 111, pp. 69-77, 1989.
13. R. Sangras, Z. Dai, G. M. Faeth, Mixing Structure of Plane Self-Preserving Buoyant Turbulent Plumes, J. Heat Transfer, vol. 120, pp. 1033-1041, 1998.
14. J. S. Turner, Buoyancy Effects in Fluids, Cambridge University Press, 1973.

15. T. J. Heindel, S. Ramadhyani, F. P. Incropera, Assessment of Turbulence Models for Natural Convection in an Enclosure, Numerical Heat Transfer, Part B,vol. 26, pp. 147-172, 1994.
16. G. Cox, Combustion Fundamentals of Fire, Academic Press, 1995.
17. W. G. Bos, T. van Den Elsen, C. J. Hoogendoorn, Comments on 'Numerical study of stratification of a smoke layer in a corridor', Combust. Sci. Technol. 46, 333, 1986.
18. P. A. Rubini, SOFIE - Simulation of Fires in Enclosures, Proceedings of 5th International Symposium on Fire Safety Science, Melbourne, Australia, IAFSS, ISBN
19. M. J. Lewis, J. B. Moss, P. A. Rubini, CFD modelling of combustion and heat transfer in compartment fires, Proceedings of 5th International Symposium on Fire Safety Science, Melbourne, Australia, March 1997, International Association for Fire Safety Science, ISBN 4-9900625-5-5.
20. H. Rouse, C. S. Yih, H. W. Humphreys, Gravitational Convection from a Boundary Source, Tellus, vol. 4, pp. 201-210, 1952.
21. W. K. Chow, W. K. Mok, CFD Fire Simulations with Four Turbulence Models and their Combinations, J. Fire Sciences, Vol. 17, pp. 209-239, 1999.

Table 1

Grid:	A	B	C	D
V	0.114	0.115	0.115	0.116
T	0.116	0.117	0.118	0.118

Table 1: Grid independence on ASMGGDH

Table 2

V spread	ORIGINAL	SGDH	GGDH	ASM	ASMSGDH	ASMGGDH
1m:2m	0.076	0.078	0.112	0.080	0.083	0.114
Source:2m	0.076	0.097	0.131	0.080	0.103	0.132
T spread						
1m:2m	0.079	0.080	0.115	0.083	0.086	0.116

Table 2: Spread rates of all models with $C_{3\varepsilon}$=0.6

Table 3

Spread rates	ORIGINAL	SGDH, C3ε=0	SGDH, C3ε=0.6
V	0.076	0.076	0.078
T	0.079	0.079	0.080

Table 3: Velocity and temperature spread rates of the SGDH model

Table 4

ASMGGDH

$C_{3\varepsilon}$	0	0.5	0.6	0.7	0.8
V	0.084	0.107	0.114	0.122	0.132
T	0.087	0.109	0.116	0.125	0.134

GGDH

$C_{3\varepsilon}$	0	0.5	0.6	0.7	0.8
V	0.080	0.104	0.112	0.122	0.134
T	0.082	0.106	0.115	0.125	0.137

Table 4: Variance with $C_{3\varepsilon}$ of spread rates.

Table 5

$C_{3\varepsilon}$	0	0.5	0.6	0.7	0.8
ASMGGDH	0.365	0.327	0.318	0.309	0.301
GGDH	0.371	0.328	0.319	0.310	0.300

Table 5: Variance with $C_{3\varepsilon}$ of centre-line velocities.

Figure 1

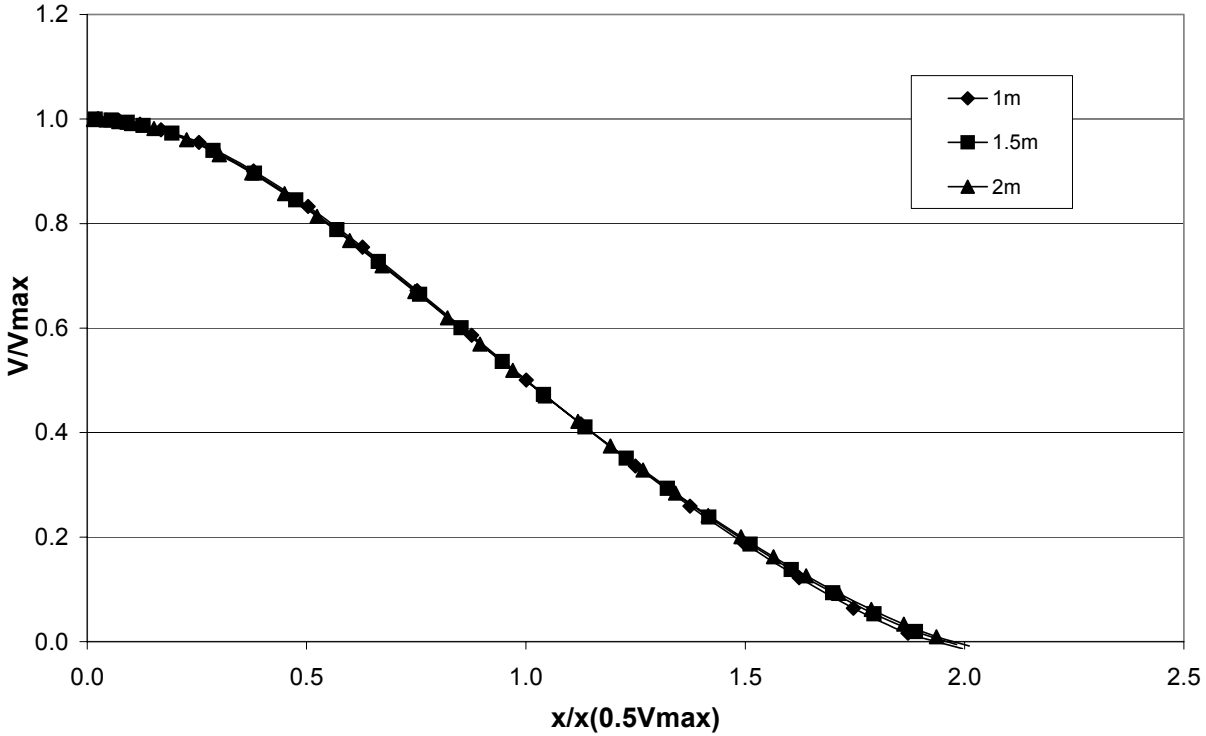

Figure 1: Normalised velocity profiles for ASMGGDH, $C_{3\varepsilon}$=0.6, at various distances from the source.

Figure 2

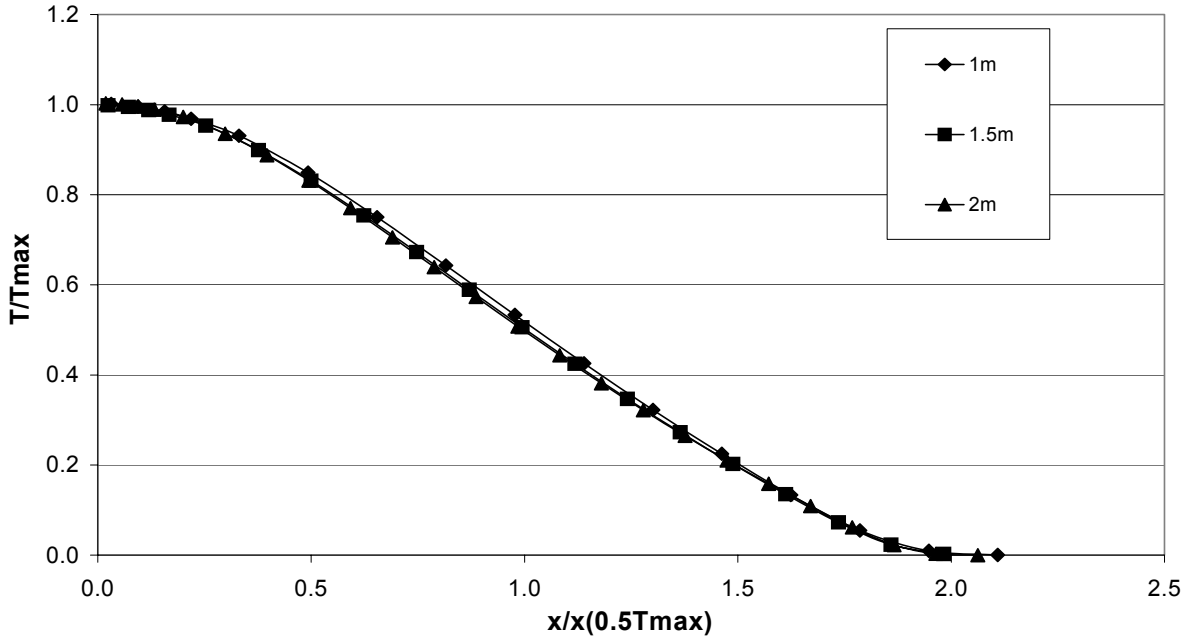

Figure 2:Normalised temperature profiles for SGDH, $C_{3\varepsilon}$=0.6, at various distances from source.

Figure 3

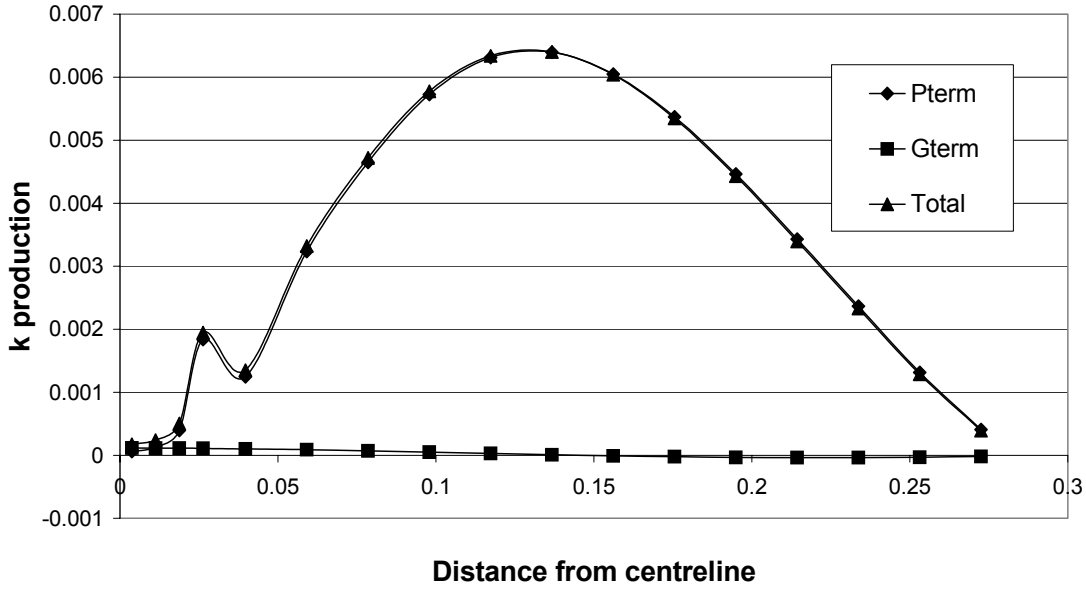

Figure 3: k production term profiles 1.5m from source for SGDH with $C_{3\varepsilon}$=0.6.

Figure 4

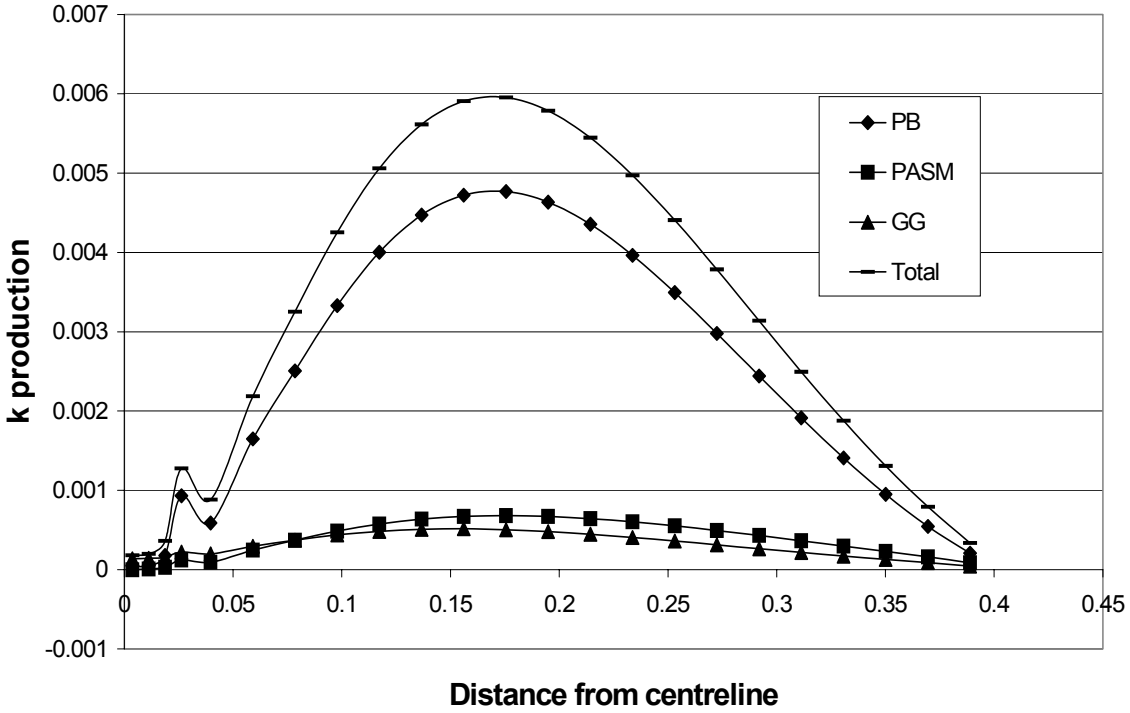

Figure 4: k production term profiles 1.5m from source for ASMGGDH with $C_{3\varepsilon}$=0.6.